

# Measuring the relative strong phase in $D^0 \rightarrow K^{*+} K^-$ and $D^0 \rightarrow K^{*-} K^+$ decays

Jonathan L. Rosner and Denis A. Suprun

*Enrico Fermi Institute and Department of Physics, University of Chicago, Chicago, Illinois 60637, USA*

(Received 16 April 2003; published 15 September 2003)

In a recently suggested method for measuring the weak phase  $\gamma$  in  $B^\pm \rightarrow K^\pm(KK^*)_D$  decays, the relative strong phase  $\delta_D$  in  $D^0 \rightarrow K^{*+} K^-$  and  $D^0 \rightarrow K^{*-} K^+$  decays (equivalently, in  $D^0 \rightarrow K^{*+} K^-$  and  $\bar{D}^0 \rightarrow K^{*+} K^-$ ) plays a role. It is shown how a study of the Dalitz plot in  $D^0 \rightarrow K^+ K^- \pi^0$  can yield information on this phase, and the size of the data sample which would give a useful measurement is estimated.

DOI: 10.1103/PhysRevD.68.054010

PACS number(s): 13.25.Ft, 14.40.Lb

The relative strong phases for charmed particle decays obey patterns which are not easily anticipated from first principles but are subject to detailed experimental study, for example through the construction of amplitude triangles based on experimentally observed decay rates [1–4]. It has also been suggested [5–7] that the final-state phase in the doubly Cabibbo-suppressed decay  $D^0 \rightarrow K^+ \pi^-$  may not be the same as that in the Cabibbo-favored decay  $D^0 \rightarrow K^- \pi^+$ , even though they should be equal in the flavor-SU(3) limit [8]. Methods for measuring their difference have been proposed [9,10]. A Dalitz-plot method for measuring the corresponding phase difference in  $D^0 \rightarrow K^{*+} \pi^-$  and  $D^0 \rightarrow K^{*-} \pi^+$  makes use of the interference between  $K^{*+}$  and  $K^{*-}$  bands in  $D^0 \rightarrow K_S^+ \pi^+ \pi^-$  and is compatible with zero strong phase difference [11,12].

Recently the question has been raised of the relative strong phase  $\delta_D$  between  $D^0 \rightarrow K^{*+} K^-$  and  $D^0 \rightarrow K^{*-} K^+$  decays (equivalently, in  $D^0 \rightarrow K^{*+} K^-$  and  $\bar{D}^0 \rightarrow K^{*+} K^-$ ) [13]. This phase is important in a proposed method for measuring the weak phase  $\gamma$  in the  $B^\pm \rightarrow (KK^*)_D K^\pm$  decays. In the present paper we point out that  $\delta_D$  may be measured very directly through the interference of  $K^{*+}$  and  $K^{*-}$  bands in  $D^0 \rightarrow K^+ K^- \pi^0$  decays [14]. We discuss the size of present and anticipated samples of this final state and indicate the attainable experimental precision for  $\delta_D$ .

We follow the notations of Ref. [13] and define the  $D$  decay amplitudes

$$\begin{aligned} A_D &\equiv A(D^0 \rightarrow K^- K^{*+}), \\ \bar{A}_D &\equiv A(\bar{D}^0 \rightarrow K^- K^{*+}), \end{aligned} \quad (1)$$

and their ratio

$$\frac{\bar{A}_D}{A_D} = r_D e^{i\delta_D}. \quad (2)$$

The weak phase of  $\bar{D}^0 \rightarrow K^- K^{*+}$  is negligible, so the  $CP$  conjugate amplitude is  $A(D^0 \rightarrow K^+ K^{*-}) = \bar{A}_D$ . We further define

$$\begin{aligned} A'_D &\equiv A(D^0 \rightarrow K^- (K^+ \pi^0)_{K^{*+}}), \\ \bar{A}'_D &\equiv A(D^0 \rightarrow K^+ (K^- \pi^0)_{K^{*-}}). \end{aligned} \quad (3)$$

The amplitudes of the  $K^{*+} \rightarrow K^+ \pi^0$  and  $K^{*-} \rightarrow K^- \pi^0$  decays are equal. Then the ratio of the amplitudes in Eqs. (3) is

$$\frac{\bar{A}'_D}{A'_D} = \frac{\bar{A}_D}{A_D} = r_D e^{i\delta_D}. \quad (4)$$

Two channels of  $D^0 \rightarrow K^+ K^- \pi^0$  go through a resonant decay of an intermediate  $K^{*+}$  or  $K^{*-}$ . They fill two bands in the Dalitz plot (see Fig. 1). The width of these bands is determined by the full width  $\Gamma \equiv \Gamma_{K^{*\pm}} = (50.8 \pm 0.9)$  MeV [15]. Namely, the left vertical line corresponds to  $m_{K^+ \pi^0}^2 = (m_{K^{*+}} - \Gamma/2)^2$ , while the right one corresponds to  $m_{K^+ \pi^0}^2 = (m_{K^{*+}} + \Gamma/2)^2$ . Analogous expressions determine the values of  $m_{K^- \pi^0}^2$  along the bottom and top borders of the horizontal band. For now we will neglect the actual Breit-Wigner distribution of event density across the bands. Instead, we will assume that the resonant decays are equally likely to appear near the central line of a band and near its borders. We will also assume that the resonant decays do not fall in the regions outside the two bands. We will neglect other resonant decays with smaller branching ratios that are not yet detected but may contribute to the Dalitz plot, such as  $D^0 \rightarrow \pi^0(K^+ K^-)_\phi$ ,  $D^0 \rightarrow \pi^0(K^+ K^-)_{a_0}$ ,  $D^0 \rightarrow \pi^0(K^+ K^-)_{f_0}$ ,  $D^0 \rightarrow K^- (K^+ \pi^0)_{K_0^{*0}(1430)^+}$ , and  $D^0 \rightarrow K^- (K^+ \pi^0)_{\kappa(800)^+}$ . Some of them are discussed later in the text and in Appendix B. Nonresonant decays uniformly fill the allowed phase space and provide a small background. For simplicity of the argument we will neglect it as well.

The square at the intersection of the bands is the region where two channels interfere with each other. We denote  $\epsilon$  to be the fraction of  $D^0 \rightarrow K^- (K^+ \pi^0)_{K^{*+}}$  decays that fall into the square region. This fraction only depends on masses and spins of particles involved in the process and the width  $\Gamma = \Gamma_{K^{*\pm}}$ . So, the probability of a  $D^0 \rightarrow K^+ (K^- \pi^0)_{K^{*-}}$  decay falling into the square region is  $\epsilon$  as well. This probability is calculated in Appendix A:  $\epsilon \approx 0.039$ .

Now we can write the number of decays detected in the square region of the Dalitz diagram:

$$\begin{aligned} N_s &\propto |\sqrt{\epsilon} A'_D + \sqrt{\epsilon} \bar{A}'_D|^2 \\ &= \epsilon (1 + 2r_D \cos \delta_D + r_D^2) |A'_D|^2, \end{aligned} \quad (5)$$

while the rest of the resonant decays contribute to the bands outside the square region:

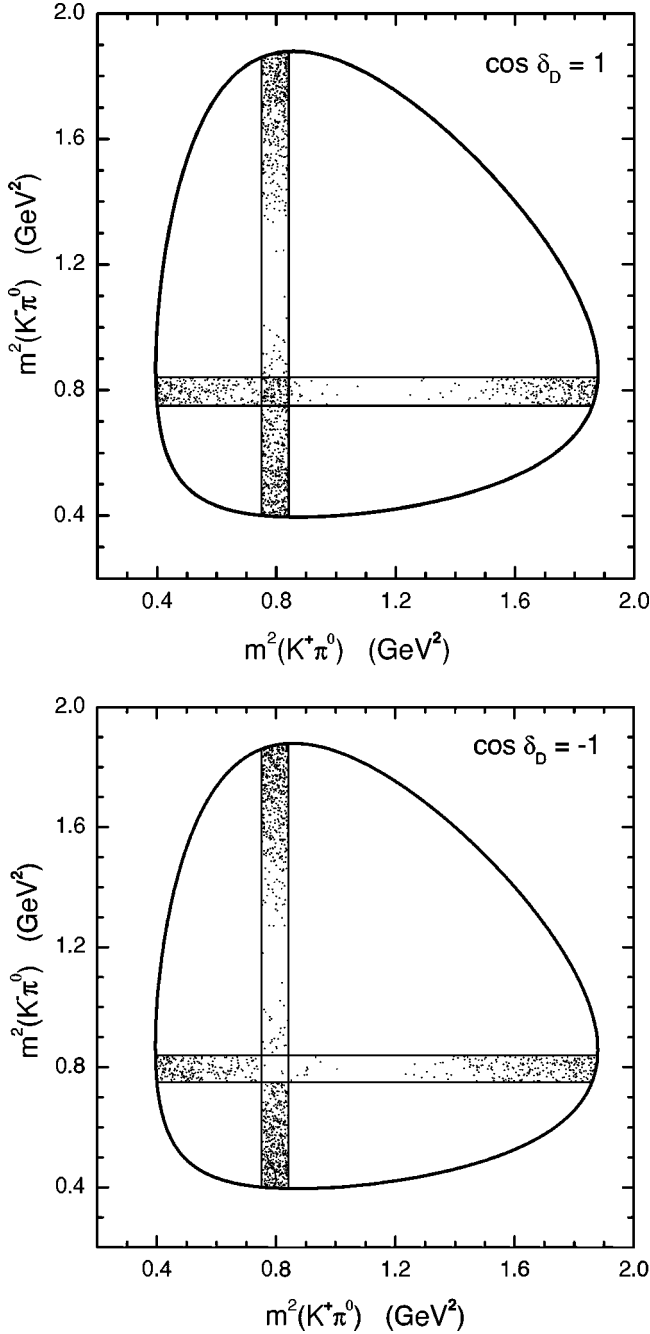


FIG. 1. The Dalitz plots of the  $D^0 \rightarrow K^+ K^- \pi^0$  decay. Top panel: constructive interference ( $\cos \delta_D = 1$ ), 113 events in the square region; bottom panel: destructive interference ( $\cos \delta_D = -1$ ), 4 events in the square region. The total number of events in the bands is  $N = 1500$  in both cases.

$$N_{out} \propto (1 - \epsilon)(|A'_D|^2 + |\bar{A}'_D|^2) = (1 - \epsilon)(1 + r_D^2)|A'_D|^2, \quad (6)$$

so that the total number of the events detected in the bands is

$$N = N_s + N_{out} \propto (1 + 2\epsilon r_D \cos \delta_D + r_D^2)|A'_D|^2. \quad (7)$$

Experimental measurements of  $N_s$  and  $N$  provide a way of measuring the strong phase  $\delta_D$ :

$$\cos \delta_D = \frac{1 + r_D^2}{2\epsilon r_D} \frac{N_s/N - \epsilon}{1 - N_s/N}. \quad (8)$$

The uncertainty in  $\epsilon$  can be neglected because it is determined by the uncertainties in particles' masses and width  $\Gamma$ , which are small. The ratio  $r_D$  defined by Eq. (2) can be calculated from the measured branching ratios:  $\mathcal{B}(D^0 \rightarrow K^+ K^{*-}) = (2.0 \pm 1.1) \times 10^{-3}$  and  $\mathcal{B}(D^0 \rightarrow K^- K^{*+}) = (3.8 \pm 0.8) \times 10^{-3}$  [15]. Assuming the uncertainties of these two measurements are uncorrelated,  $r_D = 0.73 \pm 0.21$ . These values are based on a sample of 35  $D^0 \rightarrow KK^*$  decays [16]. For a larger sample, the relative uncertainty in  $r_D$  will decrease as  $1/\sqrt{N}$ . Taking the uncertainties of the decay numbers  $N_s$  and  $N$  to be their square roots, we can calculate the uncertainty  $\sigma(\cos \delta_D)$ . One can show that the uncertainty in  $\cos \delta_D$  is mostly determined by the uncertainty in  $N_s$ :

$$\begin{aligned} \sigma(\cos \delta_D) &\approx \left| \frac{\partial \cos \delta_D}{\partial N_s} \right| \sigma(N_s) \\ &= \frac{(1 - \epsilon)(1 + r_D^2)}{2\epsilon r_D} \frac{\sqrt{N_s/N}}{(1 - N_s/N)^2} \frac{1}{\sqrt{N}}. \end{aligned} \quad (9)$$

Unlike  $\cos \delta_D$  itself, the uncertainty of this quantity depends not only on the ratio  $N_s/N$  but on the total number  $N$  of the events detected in the bands as well.

As an aside, note that Eq. (8) predicts a linear dependence of  $\cos \delta_D$  on  $Z \equiv (N_s/N)/(1 - N_s/N)$  with the slope  $S = (1 - \epsilon)(1 + r_D^2)/(2\epsilon r_D)$ . We could alternatively write Eq. (9) as

$$\begin{aligned} \sigma(\cos \delta_D) &\approx \left| \frac{\partial \cos \delta_D}{\partial Z} \right| \sigma(Z) \\ &\approx S \frac{\sqrt{N_s/N}}{(1 - N_s/N)^2} \frac{1}{\sqrt{N}}. \end{aligned} \quad (10)$$

The maximum possible value of the ratio  $N_s/N$  is achieved if the contributions from two bands are fully coherent, i.e., if  $\cos \delta_D = 1$ . In this case

$$\begin{aligned} \frac{N_s}{N} &= \left( \frac{N_s}{N} \right)_{max} \\ &= \frac{\epsilon(1 + r_D^2)}{1 + 2\epsilon r_D + r_D^2} \\ &= 0.074 \pm 0.003. \end{aligned} \quad (11)$$

The minimum possible  $N_s/N$  is a result of the fully destructive interference at  $\cos \delta_D = -1$ . Then,

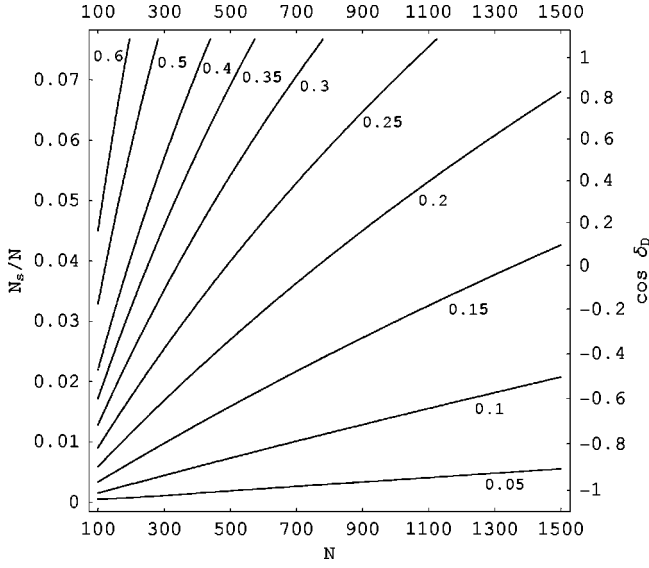


FIG. 2. Contours of  $\sigma(\cos \delta_D)$  for  $N_s/N$  between 0 and 0.077, i.e., for  $\cos \delta_D$  between  $-1.05$  and  $1.09$ .

$$\begin{aligned} \frac{N_s}{N} &= \left( \frac{N_s}{N} \right)_{\min} \\ &= \frac{\epsilon(1-r_D)^2}{1-2\epsilon r_D+r_D^2} \\ &= 0.0020 \pm 0.0035. \end{aligned} \quad (12)$$

Thus, if  $\cos \delta_D$  is close to  $-1$ , one may observe no events in the square region. The source of the uncertainties in the maximum and minimum values of the  $N_s/N$  ratio is the current 30% error in  $r_D$  which will be improved as more  $D^0 \rightarrow KK^*$  decays are detected. Within  $1\sigma$  uncertainty, we can expect the  $N_s/N$  ratio to lie between 0 and 0.077.

Figure 2 shows the contours of constant  $\sigma(\cos \delta_D)$  calculated for this region of  $N_s/N$  from Eq. (9) for the total number of band events  $N$  between 100 and 1500. The uncertainty in  $\cos \delta_D$  is an increasing function of  $N_s/N$ . So,  $\cos \delta_D$  will be measured least precisely if it is close to unity. This corresponds to a near maximum value of the  $N_s/N$  ratio. To estimate the largest uncertainty for different numbers of band events, we calculate how  $\sigma(\cos \delta_D)$  decreases with  $N$  when  $N_s/N$  is fixed at its maximum value of 0.077:

$$\sigma_{\max}(\cos \delta_D) \approx \frac{8.4}{\sqrt{N}}. \quad (13)$$

Now we discuss the consequences of the fact that the event density across a resonant decay band is not uniform but follows the Breit-Wigner distribution. The differential cross-section for any point on the Dalitz plot (see Appendix A) is

$$\begin{aligned} \frac{d^2\Gamma}{dm_{K^+\pi^0}^2 dm_{K^-\pi^0}^2} &\propto \left| \frac{A_1(m_{K^+\pi^0}, m_{K^-\pi^0})}{m_{K^+\pi^0}^2 - m_{K^*+}^2 + im_{K^*+}\Gamma} \right. \\ &\quad \left. + \frac{r_D e^{i\delta_D} A_2(m_{K^+\pi^0}, m_{K^-\pi^0})}{m_{K^-\pi^0}^2 - m_{K^*-}^2 + im_{K^*-}\Gamma} \right|^2. \end{aligned} \quad (14)$$

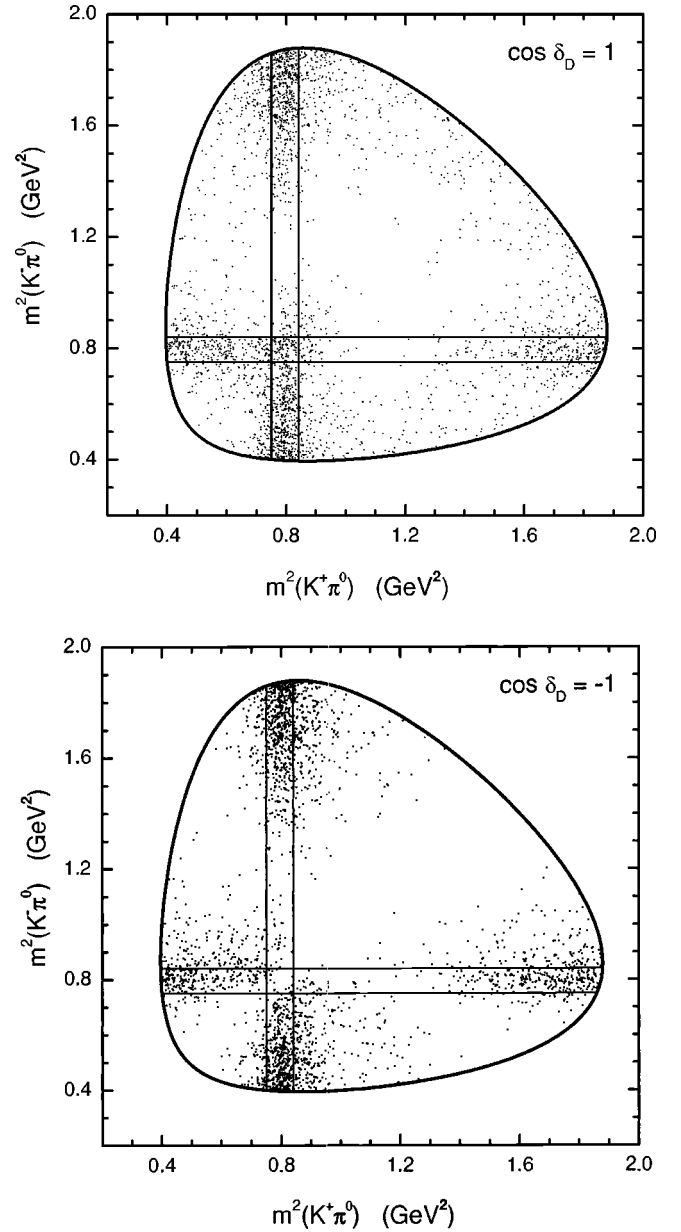


FIG. 3. Two examples of realistic Dalitz plots of the  $D^0 \rightarrow K^+ K^- \pi^0$  decay. Top panel: constructive interference ( $\cos \delta_D = 1$ ), 88 events in the square region; bottom panel: destructive interference ( $\cos \delta_D = -1$ ), 18 events in the square region. The total number of events in the bands is  $N=1500$  in both cases.

The Breit-Wigner factors in the denominators make the population density nonuniform across the bands while the kinematic factors  $A_1(m_{K^+\pi^0}, m_{K^-\pi^0})$  and  $A_2(m_{K^+\pi^0}, m_{K^-\pi^0})$  are responsible for a characteristic emptiness in the middle of the bands. The results of a Monte Carlo simulation of the distribution (14) are shown in Fig. 3.

We simulated the Dalitz plot distributions 10 times for each of 11 values of  $\cos \delta_D$  between  $-1$  and  $1$ . For the purposes of these simulations we assumed that  $r_D$  is equal to its current central value of 0.73. The plot of  $Z \equiv (N_s/N)/(1 - N_s/N)$  as a function of  $\cos \delta_D$  is shown in Fig. 4. To estimate  $\sigma(\cos \delta_D)$  we will assume that the linear relationship

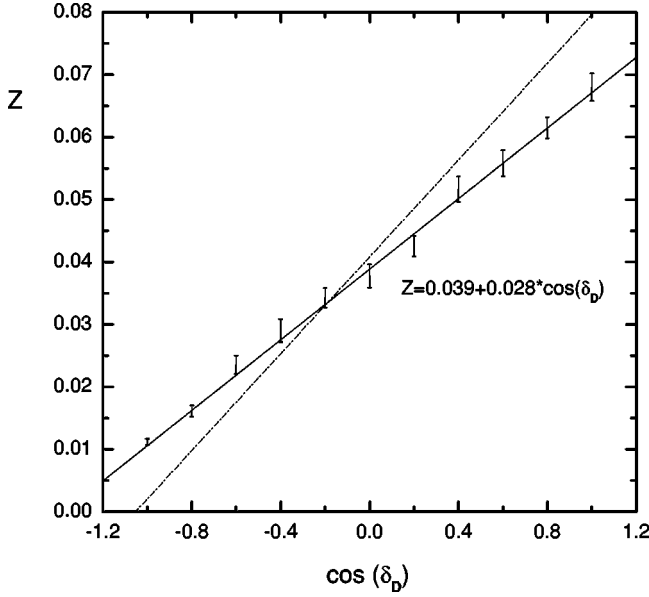


FIG. 4.  $Z \equiv (N_s/N)/(1 - N_s/N)$  as a function of  $\cos \delta_D$ . The solid line with the slope of  $0.0283 \pm 0.0005$  is the best linear fit to the results of the Monte Carlo simulations. The dash-dotted line is the prediction of the simplified model which does not take into account the Breit-Wigner resonant shapes [Eq. (8)].

between the two quantities still holds. Then, the slope is  $S = 1/(0.0283 \pm 0.0005) = 35.3 \pm 0.6$  while the maximum value of  $N_s/N$  is  $0.0637 \pm 0.0019$  at  $\cos \delta_D = 1$ . Both errors are purely statistical Monte Carlo uncertainties. These new values of the slope  $S$  and  $(N_s/N)_{\max}$  can be plugged into Eq. (10) to give our best estimate of the maximum uncertainty in  $\cos \delta_D$ :  $\sigma(\cos \delta_D) = (10.16 \pm 0.26)/\sqrt{N}$ , with the upper bound

$$\sigma_{\max}(\cos \delta_D) \approx \frac{10.4}{\sqrt{N}}. \quad (15)$$

Thus, we see that the most precise measurements will be made if  $\cos \delta_D$  is close to  $-1$ . The uncertainty of the least precise measurements (in case  $\cos \delta_D$  is unity) becomes smaller than 0.33 at  $N \approx 1000$ . Although this uncertainty is rather large, it at least allows one to distinguish  $\cos \delta_D$  from 0. The measurement of  $\cos \delta_D$  will be improved to reach the uncertainty of 0.27 or better when 1500 resonant events are detected in the bands.

In fact, 1500 resonant decays in the bands is the largest sample one can expect from CLEO-c. The CESR accelerator will operate at a center-of-mass energy of  $\sqrt{s} \sim 3.77$  GeV ( $\psi''$ ) for approximately one year. The anticipated integrated luminosity will reach  $3 \text{ fb}^{-1}$ . This corresponds to a sample of 30 million  $D\bar{D}$  pairs, with 17.5 million of them being  $D^0\bar{D}^0$  pairs. The expected sample will exceed the Mark III experiment dataset by a factor of 300. Approximately 5 million  $D^0$  and  $\bar{D}^0$  mesons will be flavor tagged [17]. The other  $D$  of a pair may decay to the  $K^+K^-\pi^0$  final state through an intermediate  $K^*$ . The branching ratios of these resonant decays are  $\mathcal{B}(D^0 \rightarrow K^+(K^-\pi^0)_{K^{*-}}) = \frac{1}{3}(2.0 \pm 1.1) \times 10^{-3}$  and  $\mathcal{B}(D^0 \rightarrow K^-(K^+\pi^0)_{K^{*+}}) = \frac{1}{3}(3.8 \pm 0.8) \times 10^{-3}$ , adding up to

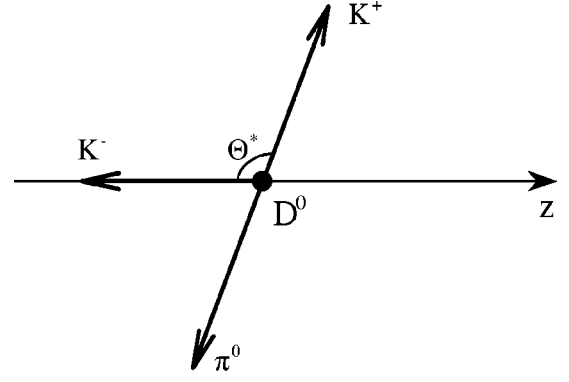


FIG. 5. The  $D^0 \rightarrow K^-(K^+\pi^0)_{K^{*+}}$  decay in the rest frame of  $K^+$  and  $\pi^0$ .

about  $2 \times 10^{-3}$ . Neglect interference effects and the number of decays should be around 10000. The estimated reconstruction efficiency for these 3-body decays is approximately 30%, so 3000 events will be detected. The Breit-Wigner distribution dictates that the bands of the Dalitz plot will be populated by half of these, i.e., by 1500 events.

The method that will be used in data analysis will likely adopt the multivariable fitting described in [18] and [19] instead of taking a close look at the number of events in the square region. We hope, however, that this paper gives a good estimate of the expected uncertainty and its dependence on the total number of detected  $D^0 \rightarrow K^+K^{*-}$  and  $D^0 \rightarrow K^-K^{*+}$  events. Other resonant decays with smaller branching ratios,  $D^0 \rightarrow \pi^0(K^+K^-)_\phi$ ,  $D^0 \rightarrow \pi^0(K^+K^-)_{a_0}$ ,  $D^0 \rightarrow \pi^0(K^+K^-)_{f_0}$ ,  $D^0 \rightarrow K^-(K^+\pi^0)_{K_0^*(1430)^+}$ , and  $D^0 \rightarrow K^-(K^+\pi^0)_{\kappa(800)^+}$ , may contribute to the Dalitz plot. The estimate of the uncertainty is most sensitive to the number of events inside the square region. Unless the bands of those decays overlap with it, they should not considerably change our estimate.

Among the five decays listed above, only those of the  $\kappa(800)^+$  have the potential to contribute to the square region. However, the  $\kappa$  is not likely to be among the intermediate states that make a significant contribution to  $D^0 \rightarrow K^-K^+\pi^0$  decays (see Appendix B). The  $\phi$  meson is a narrow vector resonance which is not much heavier than the combined mass of two charged  $K$  mesons. Therefore, it could only produce a narrow diagonal band at the very edge of the Dalitz plot. Its presence would not change the  $K^*$  band population. The same is true for  $a_0(980)$  and  $f_0(980)$  decays. They are lighter and broader (40–100 MeV) but yet not broad enough to significantly affect even the outer ends of the  $K^*$  bands. Such a possibility is present for  $K_0^*(1430)$  decays. The square region lies outside the  $K_0^*(1430)$  bands and their impact on the number of events  $N_s$  inside the square is insignificant. They can only make a relatively small contribution to the total number of band events  $N$  which would add just a small correction to the uncertainty in the strong phase  $\delta_D$ .

#### ACKNOWLEDGMENTS

We wish to thank D. M. Asner and M. Gronau for helpful correspondence. This work was supported in part by the

United States Department of Energy through Grant No. DE FG02 90ER40560.

## APPENDIX A: KINEMATICS AND DECAY AMPLITUDES

The first stage of the  $D^0 \rightarrow K^-(K^+\pi^0)_{K^{*+}}$  process is the decay of a pseudoscalar meson  $D^0$  into a pseudoscalar  $K^-$  and a (possibly off-shell) vector  $K^{*+}$ . Afterwards, the latter decays into  $K^+$  and  $\pi^0$ . From angular momentum conservation the helicity of  $K^{*+}$  is 0. The corresponding polarization vector is  $\epsilon_{K^{*+}} = \epsilon^{(\lambda=0)} = (|\mathbf{p}_{K^{*+}}|, 0, 0, E_{K^{*+}})/m_{K^+\pi^0}$  ( $m_{K^+\pi^0}$  is the invariant mass of  $K^{*+}$  and the  $z$  axis is chosen to point in the direction of the  $K^{*+}$  momentum  $\mathbf{p}_{K^{*+}}$ , see Fig. 5).

The amplitude  $A_1(m_{K^+\pi^0}, m_{K^-\pi^0})$  of the  $K^{*+} \rightarrow K^+\pi^0$  decay should be Lorentz invariant, i.e., it should contain a product of two 4-vectors. There is only one nonvanishing possibility,  $\epsilon_{K^{*+}}(p_{K^+} - p_{\pi^0})$ , since the other,  $\epsilon_{K^{*+}}(p_{K^+} + p_{\pi^0}) = \epsilon_{K^{*+}}p_{K^{*+}}$ , is identically zero. Then the former can be written in the rest frame of  $K^+$  and  $\pi^0$  as

$$A_1(m_{K^+\pi^0}, m_{K^-\pi^0}) \propto (0, 0, 0, 1)(E_{K^+}^* - E_{\pi^0}^*, 2\mathbf{p}_{K^+}^*) \\ = 2|\mathbf{p}_{K^+}^*| \cos \theta^*, \quad (\text{A1})$$

where  $\theta^*$  is the angle between the negative direction of the  $z$  axis and the direction of the  $K^+$  momentum  $\mathbf{p}_{K^+}^*$  in the rest frame of  $K^+$  and  $\pi^0$ . We will keep using the “\*” subscript for quantities determined in this frame.  $\cos \theta^*$  is given by

$$\cos \theta^* = \frac{m_{K^-\pi^0}^2 - m_{K^+}^2 - m_{\pi^0}^2 - 2E_{K^+}^*E_{\pi^0}^*}{2|\mathbf{p}_{K^+}^*||\mathbf{p}_{\pi^0}^*|}, \quad (\text{A2})$$

so

$$A_1(m_{K^+\pi^0}, m_{K^-\pi^0}) \propto \frac{m_{K^-\pi^0}^2 - m_{K^+}^2 - m_{\pi^0}^2 - 2E_{K^+}^*E_{\pi^0}^*}{|\mathbf{p}_{K^+}^*|}, \quad (\text{A3})$$

where

$$E_{K^+}^* = (m_{D^0}^2 - m_{K^+}^2 - m_{\pi^0}^2)/2m_{K^+\pi^0}, \quad (\text{A4})$$

$$E_{\pi^0}^* = (m_{K^+\pi^0}^2 - m_{K^+}^2 + m_{\pi^0}^2)/2m_{K^+\pi^0}, \quad (\text{A5})$$

$$|\mathbf{p}_{K^+}^*| = \lambda^{1/2}(m_{D^0}^2, m_{K^+}^2, m_{\pi^0}^2)/2m_{K^+\pi^0}, \quad (\text{A6})$$

$$|\mathbf{p}_{\pi^0}^*| = |\mathbf{p}_{K^+}^*|, \quad (\text{A7})$$

$$\lambda(x, y, z) \equiv x^2 + y^2 + z^2 - 2xy - 2xz - 2yz. \quad (\text{A8})$$

Including the finite resonance width  $\Gamma_{K^{*+}}$  into the  $K^{*+}$  propagator, we can write the amplitude of the  $D^0 \rightarrow K^-(K^+\pi^0)_{K^{*+}}$  decay as

$$A(D^0 \rightarrow K^-(K^+\pi^0)_{K^{*+}}) \\ \propto \frac{A_1(m_{K^+\pi^0}, m_{K^-\pi^0})}{m_{K^+\pi^0}^2 - m_{K^{*+}}^2 + im_{K^{*+}}\Gamma}. \quad (\text{A9})$$

As for the  $D^0 \rightarrow K^+(K^-\pi^0)_{K^{*-}}$  decay, its amplitude can be derived in a similar way and is equal to

$$A(D^0 \rightarrow K^+(K^-\pi^0)_{K^{*-}}) \\ \propto r_D e^{i\delta_D} \frac{A_2(m_{K^+\pi^0}, m_{K^-\pi^0})}{m_{K^-\pi^0}^2 - m_{K^{*-}}^2 + im_{K^{*-}}\Gamma}, \quad (\text{A10})$$

with the kinematic factor  $A_2$  defined as  $A_2(m_{K^+\pi^0}, m_{K^-\pi^0}) \equiv A_1(m_{K^-\pi^0}, m_{K^+\pi^0})$ . The factor  $r_D e^{i\delta_D}$  accounts for possible differences in hadronization as vector particles between quarks arising from the virtual  $W^+$  and spectator quarks.

## Calculation of the fraction $\epsilon$ of resonant decays that fall into the square region

For the particular case of an on-shell resonant  $K^{*+}$  we can neglect the Breit-Wigner denominator of Eq. (A9). In this case the amplitude of the  $D^0 \rightarrow K^-(K^+\pi^0)_{K^{*+}}$  decay is proportional to  $A_1(m_{K^+\pi^0}, m_{K^-\pi^0})$ . The kinematics of the two-body  $D^0 \rightarrow K^-K^{*+}$  and  $K^{*+} \rightarrow K^+\pi^0$  decays determine  $E_{K^+}^* = 1.37$  GeV,  $E_{\pi^0}^* = 0.32$  GeV,  $|\mathbf{p}_{K^+}^*| = 1.27$  GeV and  $|\mathbf{p}_{\pi^0}^*| = 0.29$  GeV. As a result, Eq. (A2) says

$$\cos \theta^* = 1.36(m_{K^-\pi^0}^2 - 1.135), \quad (\text{A11})$$

where  $m^2(K^-\pi^0)$  is in  $\text{GeV}^2$ . Thus, the amplitude of the  $D^0 \rightarrow K^-(K^+\pi^0)_{K^{*+}}$  decays is proportional to  $(m_{K^-\pi^0}^2 - 1.135)$ . These resonant decays fill the vertical band in a nonuniform way: no decays happen at the middle of the band where  $m_{K^-\pi^0}^2 - 1.135 = 0$ . The majority of the events will concentrate near both band ends where  $|m_{K^-\pi^0}^2 - 1.135|$  is the largest.

Now we can calculate the fraction of  $D^0 \rightarrow K^-(K^+\pi^0)_{K^{*+}}$  decays that fall into the square region,

$$\epsilon = \int_{0.75}^{0.84} (x - 1.135)^2 dx \bigg/ \int_{0.40}^{1.87} (x - 1.135)^2 dx \\ = 0.039, \quad (\text{A12})$$

where  $(m_{K^{*+}} - \Gamma/2)^2 = 0.75 \text{ GeV}^2$  and  $(m_{K^{*+}} + \Gamma/2)^2 = 0.84 \text{ GeV}^2$  are the boundaries of the square region and 0.40 and 1.87 are the boundaries of the whole band. The latter can be derived from Eq. (A11).

This simple calculation implied that the population density of the vertical band is constant along any cross section of the band, i.e., at a fixed  $m_{K^-\pi^0}^2$  it is independent of variations of  $m_{K^+\pi^0}^2$  across the band. A more precise discussion involves a simulation of the interference between the Breit-Wigner resonant shapes of Eqs. (A9) and (A10).

## APPENDIX B: INFLUENCE OF SCALAR RESONANCE $\kappa$

The existence of broad scalar resonances below 1 GeV has been a controversial issue for a long time [20]. A few experiments have been able to explore the possibility of their presence as intermediate resonant states in three-body  $D$  de-



cays. The modes that were studied include  $D^+ \rightarrow \pi^- \pi^+ \pi^+$  [19],  $D_s^+ \rightarrow \pi^- \pi^+ \pi^+$  [21],  $D^+ \rightarrow K^- \pi^+ \pi^+$  [22] (E791 Collaboration),  $D^0 \rightarrow K_S^0 \pi^+ \pi^-$  [11],  $D^0 \rightarrow K^- \pi^+ \pi^0$  [18] (CLEO), and  $D^0 \rightarrow K^0 K^- \pi^+$  [23] (BaBar). The first two studies obtained evidence for a light (478 MeV)  $\sigma$  resonance and measured the properties of the  $f_0(980)$ . The last four might provide some information on the presence of an intermediate S-wave  $K\pi$  resonance. Indeed, the E791 analysis of a Dalitz plot found that the best fit to the data is obtained allowing for the presence of an additional scalar resonance  $\kappa(800)^0$ . However, neither CLEO studies found evidence for  $\kappa^0$  or its isodoublet partner  $\kappa^+$ . The preliminary BaBar analysis saw  $\kappa$  at the level of  $1\sigma$  which does not allow the confirmation of its presence. Other types of decays could also provide a glimpse of  $\kappa$ . The BES Collaboration found  $\kappa^0$  as an intermediate state in  $J/\psi \rightarrow \bar{K}^*(892)^0 K^+ \pi^-$  decays [24], while the FOCUS Collaboration studied the interference phenomena in  $D^+ \rightarrow K^- \pi^+ \mu^+ \nu$  decays [25]. Their data can be described by  $\bar{K}^{*0}$  interference with either a constant amplitude or a broad spin zero resonance.

The  $D^0 \rightarrow K^\mp K^* \pi^\pm$  decays discussed in this paper can be affected by the possible presence of  $\kappa^\pm$  among the intermediate states. The bands of a broad  $\kappa(800)$  would cover more than 50% of the Dalitz plot, thereby interfering with the  $K^*$  bands and affecting their population. One would expect that in this case the total branching ratio of  $D^0 \rightarrow K^+ K^- \pi^0$  decays would be considerably larger than the sum of the  $D^0 \rightarrow KK^*$  modes. Indeed, in  $D^+ \rightarrow K^- \pi^+ \pi^+$  an unusually high fraction (over 90%) of decays was found to be nonresonant by previous experiments [26]. That was unusual as the nonresonant (NR) contribution in three-body decays is small

in most other cases. That was an indication of a possible broad scalar contribution and motivated the recent searches for it. It was found that the complex structure of the Dalitz plot was best explained when the  $\kappa$  presence is assumed [22]. Then, intermediate decays through the  $\kappa\pi^+$  state account for about 50% of decays while the NR fraction drops to a value of 13% more characteristic of other decays.

The present knowledge of  $D^0 \rightarrow K^\mp K^* \pi^\pm$  decays does not reveal a similar large nonresonant (or broad scalar) contribution. The current data on the resonant [15,16] and inclusive [15,27] decays come from CLEO measurements. The inclusive branching ratio is  $\mathcal{B}(D^0 \rightarrow K^+ K^- \pi^0) = (1.24 \pm 0.35) \times 10^{-3}$ . The branching ratios of the  $K\pi$  resonant decays are  $\mathcal{B}(D^0 \rightarrow K^+ (K^- \pi^0)_{K^{*-}}) = \frac{1}{3} (2.0 \pm 1.1) \times 10^{-3} = (0.67 \pm 0.37) \times 10^{-3}$  and  $\mathcal{B}(D^0 \rightarrow K^- (K^+ \pi^0)_{K^{*+}}) = \frac{1}{3} (3.8 \pm 0.8) \times 10^{-3} = (1.27 \pm 0.27) \times 10^{-3}$ . Neglecting the interference between these two channels (it affects just about 4% of these decays; see Appendix A), the two branching ratios add up to  $(1.93 \pm 0.45) \times 10^{-3}$ , consistent with the inclusive branching ratio within the current large uncertainties. Basically, there is no room for a broad scalar resonance channel. For example, it cannot negatively interfere with both halves of a  $K^*$  band. The phase variation across it would be significant ( $\approx 90^\circ$ ) for a  $K^*$  channel and much smaller for a broad  $\kappa$  one. If this channel is strong enough to cancel half the  $K^*$  decays it would contribute many times more than that outside the  $K^*$  bands. That would contradict the smallness of the inclusive branching ratio. Thus, we conclude that a broad scalar  $\kappa$ , if present, could only comprise a small fraction of  $D^0 \rightarrow K^+ K^- \pi^0$  decays and would not significantly affect the estimate of the uncertainty in the strong phase  $\delta_D$ .

- 
- [1] M. Suzuki, Phys. Rev. D **58**, 111504 (1998).
  - [2] J.L. Rosner, Phys. Rev. D **60**, 074029 (1999).
  - [3] J.L. Rosner, Phys. Rev. D **60**, 114026 (1999).
  - [4] C.-W. Chiang, Z. Luo, and J.L. Rosner, Phys. Rev. D **67**, 014001 (2003).
  - [5] A.F. Falk, Y. Nir, and A.A. Petrov, J. High Energy Phys. **12**, 019 (1999).
  - [6] S. Bergmann, Y. Grossman, Z. Ligeti, Y. Nir, and A.A. Petrov, Phys. Lett. B **486**, 418 (2000).
  - [7] H.J. Lipkin, Phys. Lett. B **494**, 248 (2000).
  - [8] L. Wolfenstein, Phys. Rev. Lett. **75**, 2460 (1995).
  - [9] Z.Z. Xing, Phys. Rev. D **53**, 204 (1996); Phys. Lett. B **372**, 317 (1996); **379**, 257 (1996); Phys. Rev. D **55**, 196 (1997); Phys. Lett. B **463**, 323 (1999).
  - [10] M. Gronau, Y. Grossman, and J.L. Rosner, Phys. Lett. B **508**, 37 (2001).
  - [11] CLEO Collaboration, H. Muramatsu *et al.*, Phys. Rev. Lett. **89**, 251802 (2002).
  - [12] BABAR Collaboration, A. Palano, in *Hadron Spectroscopy*, edited by Dmitry Amelin and Alexander M. Zaitsev, AIP Conf. Proc. No. 619 (AIP, Melville, NY, 2002), p. 53.
  - [13] Y. Grossman, Z. Ligeti, and A. Soffer, Phys. Rev. D **67**, 071301(R) (2003).
  - [14] The use of three-body  $D$  decays has been proposed by D. Atwood, I. Dunietz, and A. Soni, Phys. Rev. D **63**, 036005 (2001); and further developed by A. Giri, Y. Grossman, A. Soffer, and J. Zupan, hep-ph/0303187.
  - [15] Particle Data Group, K. Hagiwara *et al.*, Phys. Rev. D **66**, 010001 (2002).
  - [16] CLEO Collaboration, R. Ammar *et al.*, Phys. Rev. D **44**, 3383 (1991).
  - [17] CLEO Collaboration, R.A. Briere *et al.*, CLEO-c and CESR-c: A New Frontier of Weak and Strong Interactions, 2001, CLNS-01-1742.
  - [18] CLEO Collaboration, S. Kopp *et al.*, Phys. Rev. D **63**, 092001 (2001).
  - [19] E791 Collaboration, E.M. Aitala *et al.*, Phys. Rev. Lett. **86**, 770 (2001).
  - [20] E. van Beveren *et al.*, Z. Phys. C **30**, 615 (1986); S. Ishida *et al.*, Prog. Theor. Phys. **98**, 621 (1997); J.A. Oller, E. Oset, and J.R. Pelaez, Phys. Rev. D **59**, 074001 (1999); **60**, 099906(E) (1999); S.N. Cherry and M.R. Pennington, Nucl. Phys. A **688**, 823 (2001); F.E. Close and N.A. Tornqvist, J. Phys. G **28**, R249 (2002); P. Minkowski and W. Ochs, hep-ph/0209225.
  - [21] E791 Collaboration, E.M. Aitala *et al.*, Phys. Rev. Lett. **86**, 765 (2001).

- [22] E791 Collaboration, E.M. Aitala *et al.*, Phys. Rev. Lett. **89**, 121801 (2002).
- [23] BABAR Collaboration, B. Aubert *et al.*, SLAC-PUB-9320, BABAR-CONF-02-031. Contributed to 31st International Conference on High Energy Physics (ICHEP 2002), Amsterdam, The Netherlands, 2002, hep-ex/0207089.
- [24] BES Collaboration, J.Z. Bai *et al.*, hep-ex/0304001.
- [25] FOCUS Collaboration, J.M. Link *et al.*, Phys. Lett. B **535**, 43 (2002).
- [26] E691 Collaboration, J.C. Anjos *et al.*, Phys. Rev. D **48**, 56 (1993); E687 Collaboration, P.L. Frabetti *et al.*, Phys. Lett. B **331**, 217 (1994).
- [27] CLEO Collaboration, D.M. Asner *et al.*, Phys. Rev. D **54**, 4211 (1996).